

---

# In Vivo Measurement of D<sub>2</sub> Receptor Density and Affinity for <sup>18</sup>F-(3-*N*-Methyl)Benperidol in the Rat Striatum with a PET System for Small Laboratory Animals

Susanne Nikolaus, PhD<sup>1</sup>; Rolf Larisch, MD<sup>1</sup>; Markus Beu, BSc<sup>1</sup>; Karl Hamacher, PhD<sup>2</sup>; Farhad Forutan, BSc<sup>1</sup>; Henning Vosberg, MD<sup>1</sup>; and Hans-Wilhelm Müller, MD<sup>1</sup>

<sup>1</sup>Nuklearmedizinische Klinik, Universitätsklinikum Düsseldorf, Düsseldorf, Germany; and <sup>2</sup>Institut für Nuklearchemie, Forschungszentrum Jülich GmbH, Jülich, Germany

---

A recent investigation showed that intracerebral radioactivity concentrations can reliably be quantified in vivo with a small-animal PET device. The purpose of the current study was to investigate the binding characteristics of the D<sub>2</sub> receptor radioligand <sup>18</sup>F-(3-*N*-methyl)benperidol (<sup>18</sup>FMB) in rat striatum by determining receptor density (B<sub>max</sub>) and affinity (K<sub>d</sub>) in vivo. For validation, K<sub>d</sub> and B<sub>max</sub> additionally were determined in vitro using storage phosphor autoradiography. **Methods:** Striatal radioactivity was measured with PET in 8 Sprague–Dawley rats after injection of <sup>18</sup>FMB in increasing specific activities. Free radioligand concentrations were estimated from cortical radioactivity concentrations and were subtracted from striatal radioactivity concentrations to obtain specific binding. In vitro saturation experiments were performed on 7 further rats according to the isotopic dilution method. Specific binding was determined by both subtraction of <sup>18</sup>FMB binding in the presence of raclopride and subtraction of cortical radioactivity concentrations from total radioligand binding. Saturation binding curves were obtained by plotting specifically bound radioligand concentrations against free radioligand concentrations and were evaluated with regression analysis. **Results:** PET yielded a K<sub>d</sub> of 6.2 nmol/L and a B<sub>max</sub> of 16 fmol/mg for the striatal D<sub>2</sub> receptor. In vitro, K<sub>d</sub> and B<sub>max</sub> amounted to 4.4 nmol/L and 84.1 fmol/mg (subtraction of <sup>18</sup>FMB binding in the presence of raclopride), respectively, and 7.9 nmol/L and 70.1 fmol/mg (subtraction of cortical radioactivity concentrations), respectively. **Conclusion:** K<sub>d</sub> values measured with PET and autoradiography agreed and corresponded to inhibition constants obtained in previous in vitro studies. B<sub>max</sub> values lay within the same order of magnitude. The results of in vitro saturation binding analyses also agreed, irrespective of the mode of determination of free radioligand concentrations. Thus, B<sub>max</sub> and K<sub>d</sub> may be determined with PET in analogy to the evaluation of in vitro binding data by regression analysis of bound-versus-free ligand concentrations. Our results show that small-animal tomographs are valuable

tools for the in vivo characterization of receptor radioligands as an alternative to autoradiography.

**Key Words:** <sup>18</sup>F-(3-*N*-methyl)benperidol; dopamine D<sub>2</sub> receptors; animal PET; autoradiography; saturation binding analysis

**J Nucl Med 2003; 44:618–624**

---

**I**n a recent study, a small-animal tomograph (*1*) was validated for the performance of receptor imaging studies. We previously showed that the dopamine D<sub>2</sub> receptor radioligand <sup>18</sup>F-(3-*N*-methyl)benperidol (<sup>18</sup>FMB) accumulated within the D<sub>2</sub> receptor-rich striatal tissue and that striatal radioactivity concentrations measured in the same rats in vivo with PET and ex vivo with storage phosphor autoradiography exhibited a significant positive correlation (2). The purpose of the present study was to show the feasibility of receptor binding studies by quantifying striatal D<sub>2</sub> receptor density (B<sub>max</sub>) and binding affinity (K<sub>d</sub>) with our imaging tool and the radioligand in question.

Previous studies of D<sub>2</sub> receptor binding with small-animal tomographs either presented a descriptive analysis of striatal and cerebellar time-activity curves and striatocerebellar uptake ratios or quantified the binding potential B<sub>max</sub>/K<sub>d</sub> using reference tissue compartment models (3–9). However, the determination of K<sub>d</sub> and B<sub>max</sub> as separate values is of special relevance for the preclinical evaluation of novel radioligands. Hence, we propose an in vivo method that applies saturation binding analysis and thus allows the determination of K<sub>d</sub> and B<sub>max</sub> with PET in analogy to in vitro experiments. An in vivo Scatchard analysis has been previously performed by Tsukada and collaborators as a complement to PET to clarify whether the observed effect on receptor binding was mediated by a change of K<sub>d</sub> or B<sub>max</sub> (5). In contrast to their approach, we addressed the question of whether the classic saturation binding analysis is also valid under in vivo conditions and compared in vivo results

Received Jun. 10, 2002; revision accepted Nov. 14, 2002.

For correspondence or reprints contact: Rolf Larisch, MD, Nuklearmedizinische Klinik, Universitätsklinikum Düsseldorf, Moorenstrasse 5, 40225, Düsseldorf, Germany.

E-mail: Rolf.Larisch@uni-duesseldorf.de

with  $B_{\max}$  and  $K_d$  values obtained with conventional in vitro receptor autoradiography.

## MATERIALS AND METHODS

### Animals

Fifteen male Sprague–Dawley rats (Charles River, St. Aubin-les-Elbeuf, France) weighing between 300 and 500 g were investigated. Eight animals were examined with PET, and 7 animals were subjected to storage phosphor autoradiography. The experiment was performed in accordance with the German Law on the Protection of Animals and was approved by the regional authorities.

### Radiochemistry

$^{18}\text{F}$ MFB was synthesized as previously described (10). Nucleophilic aromatic fluorination through an  $^{18}\text{F}$ -for-nitro exchange was performed according to the method described for the butyrophe- none ligand  $^{18}\text{F}$ -(*N*-methyl)-spiperone (11). The radiochemical purity was higher than 98% as determined with high-performance liquid chromatography.  $^{18}\text{F}$ MFB is rapidly metabolized in the periphery (12). Thereby, chromatographic analysis suggests that only polar metabolites are formed, which do not partition into the brain (13). In the in vivo experiment, specific activity at injection time covered 1 order of magnitude (range,  $>11$  to  $>100$  TBq/mmol [ $>311$  to  $>2,730$  Ci/mmol]). The molar amounts of injected radioligand ranged from 0.81 to 0.54 nmol.

### PET Measurements

**Instrumentation.** The small-animal tomograph was developed by the Zentrallabor für Elektronik, Forschungszentrum Jülich GmbH, Jülich, Germany. Technical specifications have been described in detail elsewhere (1). Axial as well as transaxial field of view have a diameter of 40 mm. The sensitivity is 3.24 cps/kBq for a center–detector distance of 80 mm. The resolution is 2.1 mm (full width at half maximum). One cps/mm<sup>3</sup> as registered with the PET camera corresponds to 444 Bq/mm<sup>3</sup> (2); this value served as a calibration factor to calculate radioactivity concentrations from the count rates within the regions of interest (ROIs).

**Protocol.** After short-time inhalation anesthesia with isoflurane, the animals received intramuscular injections of ketamine (concentration, 100 mg/mL; dose, 0.9 mL/kg) and xylazine (concentration, 0.02 mg/mL; dose, 0.4 mL/kg).  $^{18}\text{F}$ MFB (mean  $\pm$  SD,  $70.4 \pm 8.7$  MBq) was diluted in 0.9% saline containing 10% ethanol and injected into the right jugular vein. The mean injection volume was  $1 \pm 0.5$  mL, and the mean injected radioactivity dose amounted to  $158.3 \pm 24.2$  MBq/kg.

After surgical dressing, the animals were positioned on the object tablet with an associated acrylic head holder comprising ear bars and tooth bars. The head holder (Institut für Medizin, Forschungszentrum Jülich GmbH) allows both the fixation and the accurate and consistent positioning of the rat head. Then, the motor-controlled object tablet was moved along the *x*-, *y*-, and *z*-axes such that the striata were localized in the center of the field of view. During scanning of the brain, the animals' bodies were kept within a lead tube (wall thickness, 20 mm) to reduce perturbations due to scattered photons. The tube was constantly perfused by warm water to maintain a body temperature of 37°.

Images were acquired over 36 min (6 time frames of 6 min each) with angular steps of 7.5° (30 s per angular step). The mean delay between application of the radioligand and start of the measurement amounted to  $8.1 \pm 4.4$  min. The data acquisition and pro-

cessing were described in detail elsewhere (1). Image reconstruction was performed in consecutive slices of 2-mm thickness.

**Evaluation.** The 6 time frames were summed, and the resulting image was analyzed with the Multi Purpose Imaging Tool (version 2.57; Advanced Tomo Vision, Erfstadt, Germany). According to the standard rat brain atlas by Paxinos and Watson (14), striata were localized individually for each animal on coronal sections. Two standard circular ROIs with diameters of 2.5 mm were drawn around the centers of both striata. The positions but not the sizes of the ROIs were adjusted individually for each animal.

According to the late-time method (15), the mean left and right striatal radioactivity concentrations in the last 3 time frames were computed and corrected for partial-volume and spillover effects from the retroorbitally situated Harder's glands, as previously described (16). From the striatal radioactivity concentrations (MBq/mm<sup>3</sup>) and the known specific activity at the beginning of the fourth time frame, the molar radioligand concentrations (fmol/mg) were computed.

On the basis of previous autoradiographic studies (17,18), cortical rather than cerebellar radioactivity concentrations were regarded as an estimation for nonspecific radioligand binding in brain tissue. Because of possible contributions of adjacent tissues to cortical radioactivity measurement, cortical receptor densities may not be obtained by simply drawing ROIs on coronal or transversal slices. To estimate the various amounts of spillover, gaussian model functions were fitted to the line activity profiles through retroorbital tissue, striatum, and adjacent occipital cortex (Fig. 1 (16)). From the cortical radioactivity concentrations (MBq/mm<sup>3</sup>) and the known specific activity at the beginning of the fourth time frame, the molar radioligand concentrations (fmol/mg) were calculated. For each animal, the cortical molar concentrations were subtracted from the striatal radioligand concentrations to obtain specific binding. Left and right striatal values of specific binding were averaged and plotted against the free radioligand concentrations.  $K_d$  and  $B_{\max}$  values were determined by means of nonlinear regression analysis using Prism (version 3.0; GraphPad Software, San Diego, CA) for Windows (Microsoft, Redmond, WA). The SDs of kinetic parameters derived by nonlinear regression analysis represent functions of the degrees of freedom, the distance of the measured points from the curves, and the overall shape of the curves. We additionally report the coefficient of variation (%CV) as a measure of identifiability of the parameters. The goodness of fit was quantified by the correlation coefficient  $R^2$ .  $R^2$  was computed by dividing the sum of squares of the vertical distances of the measured points from the best-fit curve by the sum of squares of the distances of the measured points from a horizontal line through the mean of all *y*-values. Furthermore, data were linearized by Scatchard transformation and subjected to linear regression analysis.  $B_{\max}$  and  $K_d$  values were reported; additionally, means and SDs of slope and *y*-intercept were rendered. The goodness of fit was quantified by the correlation coefficient  $r^2$ .

### In Vitro Autoradiography

**Preparation.** Upon inhalation anesthesia with isoflurane, the rats were killed by cervical dislocation. The brains were removed and frozen in isopentane ( $-70^\circ\text{C}$ ). Coronal cryosections (CM3050; Leica Camera AG, Solms, Germany) of 20- $\mu\text{m}$  thickness were made between 2.2 mm in front of and 2.3 mm behind bregma (14). Slices were mounted on microscopic slides that had been incubated with L-polylysine for 20 min and dried overnight at room temperature. Slices were air dried and stored at 4°C–8°C.

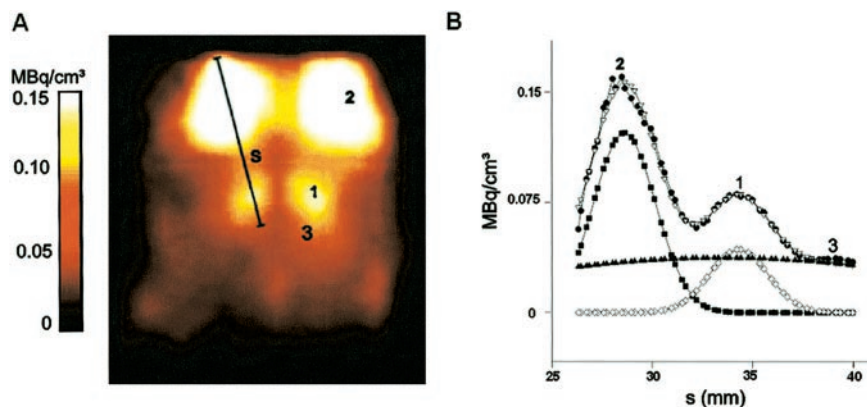


**FIGURE 1.** (A) Characteristic transversal slice of Sprague–Dawley rat head, obtained with PET camera. (B) To estimate influence of retroorbital radioactivity on determination of striatal radioactivity concentrations, gaussian model functions ( $\nabla$ ) were fitted to line activity profiles (s) ( $\bullet$ ) of both striata (1) and orbitae (2) of each side. After decomposition of sum function into the 3 components striatal ( $\diamond$ ), retroorbital ( $\blacksquare$ ), and background radioactivity ( $\blacktriangle$ ), overlap between striatal and orbital curve was taken as measure for spillover. Cortical radioactivity (3) was used to estimate free and nonspecific binding. For each animal, mean cortical values were subtracted from striatal radioactivity concentrations as averaged over time frames 4–6.

**Storage Phosphor Screen Imaging.** Slide-mounted tissues were incubated at room temperature for 60 min with 0.36 nmol/L of  $^{18}\text{FMB}$  (in routine productions, usually  $>75$  TBq/mmol [2,000 Ci/mmol]) and increasing concentrations (0–100 nmol/L) of unlabeled (3-*N*-methyl)benperidol in 50 mmol/L Tris-HCl buffer (pH, 7.4) containing 120 mmol/L NaCl, 5 mmol/L KCl, 2 mmol/L CaCl dihydrate, 1 mmol/L  $\text{MgCl}_2$  hexahydrate, and 0.2  $\mu\text{mol/L}$  idazoxan hydrochloride. After incubation, slides were washed twice for 5 min each time in ice-cold buffer followed by a quick dip into bidistilled water before being dried in a stream of cold air. In vivo, specific binding was determined by subtraction of free, that is, cortical, radioligand concentration. Here, for the purpose of validation, specific binding first was determined by joint incubation with the radioligand and 10  $\mu\text{mol/L}$  of raclopride. Second, in analogy to the evaluation of the PET images, cortical radioactivity was regarded as an estimation for nonspecific binding. Radioactivity standards were prepared from bovine brain with increasing concentrations of  $^{18}\text{FMB}$  (37–740 kBq/g of tissue, wet weight). Upon manual homogenization of the tissue, cryosections of 20- $\mu\text{m}$  thickness were made.

The principle of storage phosphor screen imaging has been described in detail elsewhere (19). In brief, imaging plates coated with photostimulable europium-doped BaFBr crystals (SR 2025; Fuji Photo Film Co., Ltd., Tokyo, Japan) were exposed to striatal slices and to standards for 17 h. Upon exposure, the plates were scanned with a high-performance imaging plate reader (BAS5000; Fuji Photo Film Co., Ltd.) providing a spatial resolution of 25  $\mu\text{m}$ . The images resulting from analog–digital conversion of the emitted luminescence were analyzed with dedicated software (TINA 2.10f; Raytest Isotopenmeßgeräte GmbH, Straubenhardt, Germany). Thereby, circular ROIs were drawn into the frontoparietal cortical region and the center of the striatal outline ( $1.36 \pm 0.4$  mm<sup>2</sup> and  $2.5 \pm 1.6$  mm<sup>2</sup>, respectively).

**Evaluation.** For each animal, left and right striatal and cortical radioactivity accumulations per square millimeter were averaged and converted into radioligand concentrations (fmol/mg of tissue, wet weight). Contingent on subtraction of the nonspecific binding, radioligand concentrations were averaged over animals for each molar concentration of the incubation solution, and SDs of the

means were computed (0.36–5.36 nmol/L;  $n = 6$ ; 10.36–50.36 nmol/L;  $n = 5$ ; 100.36 nmol/L;  $n = 4$ ). From the resulting saturation binding curves,  $K_d$  and  $B_{\text{max}}$  values were determined by means of nonlinear regression analysis. The goodness of fit was quantified by the correlation coefficient  $R^2$ . Additionally, data were displayed as Scatchard plots and subjected to a linear regression analysis.  $B_{\text{max}}$  and  $K_d$  values were reported; additionally, means and SDs of slope and y-intercept were rendered. The goodness of fit was quantified by the correlation coefficient  $r^2$ .

## RESULTS

### PET

The mean striatal radioactivity concentration was  $0.36 \pm 0.12$  kBq/mm<sup>3</sup>. Striatal ligand concentration amounted to  $18.3 \pm 9.8$  fmol/mg. After subtraction of the free ligand concentration ( $7.9 \pm 4.3$  fmol/mg), mean specific binding was  $10.3 \pm 5.7$  fmol/mg, with values ranging from 2.1 to 21.3 fmol/mg. There was a linear relationship between the injected molar amount of  $^{18}\text{FMB}$  and the cortical (free) radioligand concentration ( $r = 0.72$ ).

Nonlinear regression analysis performed with these data and the occipital radioligand accumulation as the concentration parameter yielded a  $K_d$  of 6.2 nmol/L (SD, 3.8 nmol/L; %CV, 61.3) and a  $B_{\text{max}}$  of 16 fmol/mg (SD, 4.7 fmol/mg; %CV, 29.4; Fig. 2).  $R^2$  amounted to 0.76. In the inset of Figure 2, data are displayed after linearization. Regression analysis of the Scatchard plot yielded  $K_d$  and  $B_{\text{max}}$  values of 5 nmol/L and 15.3 fmol/mg, respectively (slope,  $-0.2 \pm 0.1$ ; y-intercept,  $3 \pm 0.9$  fmol/mg). The correlation coefficient  $r^2$  was 0.43.

### Autoradiography

The mean striatal radioactivity concentrations measured with in vitro storage phosphor autoradiography amounted to  $0.5 \pm 0.2$  kBq/mm<sup>3</sup>. The means of the total striatal ligand concentrations ( $^{18}\text{FMB}$  + cold ligand) lay between 9.6  $\pm$

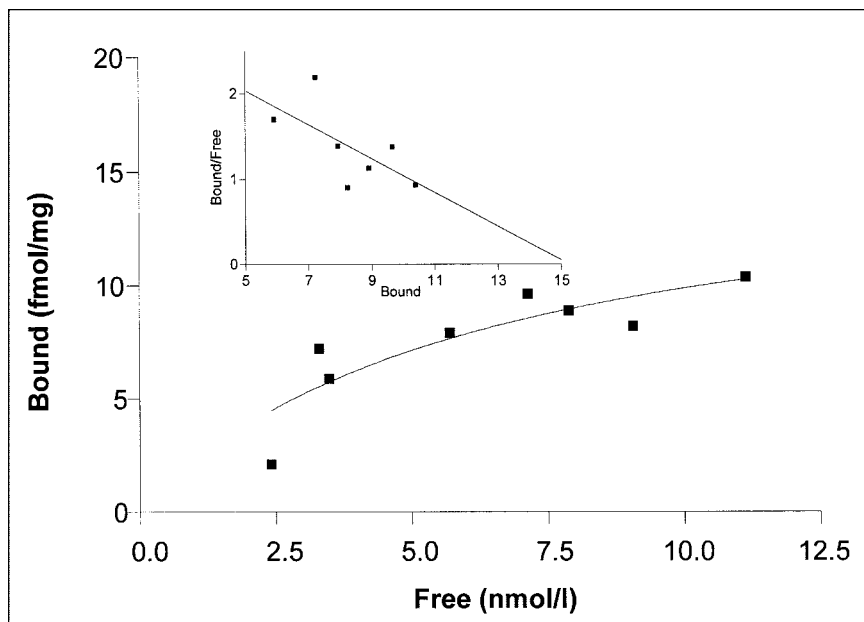


**FIGURE 2.** Nonlinear regression analysis of  $^{18}\text{FMB}$  binding to striatal dopamine  $D_2$  receptors ( $K_d$ , 6.2 nmol/L;  $B_{\max}$ , 16.03 fmol/mg). Binding data were acquired on 8 Sprague–Dawley rats with animal PET device. Free radioligand concentration in occipital cortex was used as concentration parameter. Scatchard analysis contingent on linear transformation (inset) yielded  $K_d$  and  $B_{\max}$  values of 5 nmol/L and 15.3 fmol/mg, respectively.

1.1 fmol/mg (incubation solution, 0.36 nmol/L) and  $1.4 \pm 0.1$  pmol/mg (incubation solution, 100.36 nmol/L). After subtraction of the striatal benperidol binding in the presence of raclopride, mean specific bindings between  $5 \pm 1.8$  fmol/mg (incubation solution, 0.36 nmol/L) and  $75.2 \pm 49.6$  fmol/mg (incubation solution, 100.36 nmol/L) were obtained. When cortical benperidol binding was subtracted to determine specific binding, mean values lay between  $4.4 \pm 0.8$  fmol/mg (incubation solution, 0.36 nmol/L) and  $154.2 \pm 95.7$  fmol/mg (incubation solution, 100.36 nmol/L).

Nonlinear regression analysis performed with specific binding data obtained from subtraction of benperidol binding in the presence of raclopride (Fig. 3A) yielded a  $K_d$  of 4.4 nmol/L (SD, 2.1 nmol/L; %CV, 47.7) and a  $B_{\max}$  of 84.1 fmol/mg (SD, 10.98 fmol/mg; %CV, 13.1).  $R^2$  amounted to 0.98. In the inset of Figure 3A, data are displayed as a Scatchard plot ( $K_d$ , 7.1 nmol/L;  $B_{\max}$ , 102.4 fmol/mg; slope,  $-0.1 \pm 0.05$ , y-intercept,  $14.4 \pm 2.2$  fmol/mg;  $r^2 = 0.68$ ).

Nonlinear regression analysis after determination of specific striatal binding by subtraction of cortical radioactivity concentrations (Fig. 3B) yielded a  $K_d$  of 7.9 nmol/L (SD, 1.2; %CV, 15.2) and a  $B_{\max}$  of 70.1 fmol/mg (SD, 3.8 fmol/mg; %CV, 5.4).  $R^2$  amounted to 0.998. After linearization,  $K_d$  and  $B_{\max}$  values of 5.6 nmol/L and 63 fmol/mg, respectively, were obtained (slope,  $-0.18 \pm 0.04$ ; y-intercept,  $11.2 \pm 1.3$  fmol/mg;  $r^2 = 0.83$ ; inset of Fig. 3B).

## DISCUSSION

The present investigation demonstrated specific labeling of the striatal  $D_2$  receptors of the rat by  $^{18}\text{FMB}$ .  $K_d$  and  $B_{\max}$  values of the radioligand as obtained in vivo with PET and in vitro with storage phosphor autoradiography amounted to 6.2 and 4.4 nmol/L and 16 and 84 fmol/mg, respectively.

Data also corresponded when, in analogy to the PET evaluation, cortical benperidol binding instead of striatal benperidol binding in the presence of raclopride was regarded as a measure of nonspecific binding ( $K_d$ , 7.9 nmol/L;  $B_{\max}$ , 70 fmol/mg). Irrespective of methodologic differences, saturation binding analyses in the way they were performed here led to similar results as to the  $K_d$  and results within the same order of magnitude as to the  $B_{\max}$ . This agreement of values provides the first evidence that  $K_d$  and  $B_{\max}$  can be measured with dedicated animal PET devices in the living brain in analogy to in vitro saturation binding studies.

The  $K_d$  values determined in our experiment with PET and with storage phosphor autoradiography correspond to inhibition constant ( $K_i$ ) values previously obtained for  $^{18}\text{FMB}$  and other benperidol analogues with homogenized primate ( $K_i$ , 3.6 nmol/L) and rat striata ( $K_i$ , 5.2 nmol/L) (10,20,21). This correspondence of values is remarkable given the variety of species and methods, that is, in vivo PET and in vitro autoradiography of rat striatal slices, and membrane homogenate studies on rat and primate tissues, respectively. Additionally, the in vitro assessment of  $K_i$  in the cited studies (10,20) required an entirely different experimental paradigm using  $^{18}\text{FMB}$  as a competitor against spiperone binding, whereas in our in vitro study the  $K_d$  of  $^{18}\text{FMB}$  was determined against competition with raclopride.

In the present study, cortical rather than cerebellar radioactivity concentration was used as an estimation of free and nonspecific radioligand binding. As previous autoradiographic studies have shown, both cerebellar and cortical  $D_2$  receptor densities are negligible, with  $B_{\max}$  values amounting to 1 and 0.4 fmol/mg, respectively (17). Because of the low  $D_2$  receptor concentration and the lack of anatomic landmarks, it is difficult, however, to delineate cerebellar ROIs in a reproducible manner. In contrast, cortical radio-

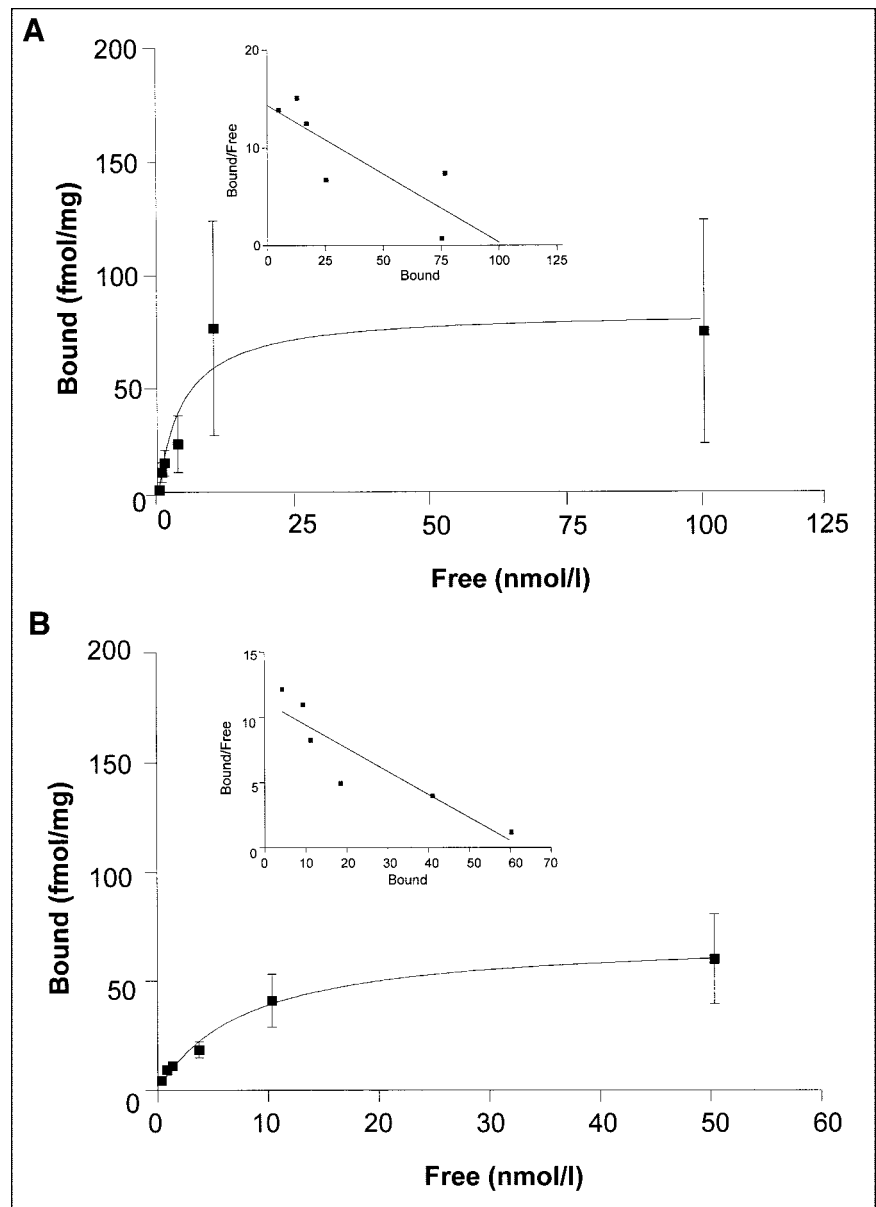


**FIGURE 3.** Saturation binding analysis of  $^{18}\text{FMB}$  binding to striatal dopamine  $\text{D}_2$  receptors. Nonspecific binding was estimated from joint incubation with  $^{18}\text{FMB}$  and highly selective competitor raclopride ( $10\ \mu\text{mol/L}$ ) (A) and in analogy to saturation binding analysis of in vivo data from cortical radioactivity concentrations (B). Binding data were acquired in vitro on striatal slices on 4–6 animals per molar concentration. (A) Nonlinear regression analysis yielded  $K_d$  of  $4.4\ \text{nmol/L}$  and  $B_{\text{max}}$  of  $84.1\ \text{fmol/mg}$ . Scatchard analysis contingent on linear transformation (inset) yielded  $K_d$  and  $B_{\text{max}}$  values of  $7.1\ \text{nmol/L}$  and  $102.4\ \text{fmol/mg}$ , respectively. (B) Nonlinear regression analysis yielded  $K_d$  of  $7.9\ \text{nmol/L}$  and  $B_{\text{max}}$  of  $70.1\ \text{fmol/mg}$ . After linearization (inset),  $K_d$  and  $B_{\text{max}}$  values of  $5.6\ \text{nmol/L}$  and  $63\ \text{fmol/mg}$ , respectively, were obtained.

activity concentrations may be determined on the same slices used for striatal ROI definition, prompting us to use the cortex as a reference region in our in vivo investigation. Moreover, we decided to use the occipitocortical region, since previous investigations have shown that occipital  $\text{D}_2$  receptor concentrations fall short of frontal ones by approximately one third (18). Because occipital  $\text{D}_2$   $B_{\text{max}}$  is that low, radioactivity concentrations in this region provided a reasonable estimation of free and nonspecific radioligand concentrations in brain tissue.

In our study,  $K_d$  values agreed irrespective of whether in vivo or in vitro saturation binding analyses were performed. Thereby, the main procedural difference lay in the determination of specific binding. In the autoradiographic study, this determination was accomplished by joint incubation of  $\text{D}_2$  receptor-rich tissue with  $^{18}\text{FMB}$  and the selective ligand

raclopride in a micromolar concentration. In vivo, the cortical radioactivity concentration was considered as an estimation for nonspecific and free radioligand binding and was subtracted from the striatal radioactivity concentrations to obtain specific binding. Thereby, the assumption of interchangeability of nonspecific and free compartment is based on the standard model for radiotracer kinetics (22). For the sake of comparability, the in vivo estimation of specific binding was also applied to autoradiographic data. Determination of specific binding in the striatum by subtraction of cortical binding instead of striatal binding in the presence of raclopride led to similar results. Also, in vivo and in vitro  $K_d$  values, both determined with the cortex as the nonspecific and free compartment, agreed.

In the previous in vitro investigations with  $^{18}\text{FMB}$  and analogues (10,20,21), no  $B_{\text{max}}$  values were reported. In our

study, the kind of estimation of nonspecific binding produced no effect on the results of in vitro saturation binding analysis: Determination of specific binding by subtraction of radioligand binding in the presence of raclopride resulted in a  $B_{\max}$  of 84 fmol/mg, whereas with cortical subtracted from striatal binding a  $B_{\max}$  of 70 fmol/mg was obtained. In the in vivo saturation binding analysis,  $B_{\max}$  was considerably lower though still within the same order of magnitude. Similar results have been reported by Hume et al. as to the intracerebral radioactivity concentration obtained with PET and with a  $\gamma$ -counter after postmortem dissection (23).

Not only the goodness of fit, with  $R^2$  values of 0.76 and 0.98 for in vivo and in vitro data, respectively, but also the degree of variation differed between methods. The %CVs obtained with nonlinear regression analysis were higher for  $K_d$  and  $B_{\max}$  values determined with PET (61% and 29.4%, respectively) than for  $K_d$  and  $B_{\max}$  values determined with storage phosphor autoradiography (48% and 13%, respectively). When cortical benperidol binding was regarded as a measure for nonspecific binding, %CVs were even lower. One possible explanation is that only 1 animal per injected molar concentration was measured with PET, whereas in the autoradiographic experiment 4–6 animals per molar concentration were entered into the nonlinear regression analysis. Thereby, in the autoradiographic experiment the fit was improved by the larger group size as such and not by the fact that  $K_d$  and  $B_{\max}$  were fitted to the means and SDs instead of to the individual values: When regression analysis was performed with the individual striatal ligand concentrations,  $K_d$  and  $B_{\max}$  values of 5.07 nmol/L and 87.11 fmol/mg, with SDs of 5.66 nmol/L and 33.83 fmol/mg, respectively, and variation coefficients of 46% and 16%, respectively, were obtained. That is, results remained within the same range also when this mode of evaluation was chosen for storage phosphor autoradiography.

When in vivo and in vitro measurements are compared, various points have to be considered. In both approaches, the mean free ligand concentration in tissue is assumed to be equal to the true free ligand concentration in the vicinity of the binding sites. We do not know whether, in either approach, this assumption is violated. First, in vivo, the cortical radioactivity concentration is considered as an estimation for the free compartment irrespective of any, even if only negligible, specific (e.g., 17,18) or nonspecific binding. Second, in vitro, the radioligand concentration in the incubation solution represents merely an estimation of the free intercellular radioligand concentration. Here, the true free radioligand concentration may be influenced by the diffusion of molecules into the brain tissue—diffusion that, apart from external conditions such as temperature, in turn depends on the degree of cellular destruction in the cryosections. Moreover, in the in vitro experiment, no nonspecifically bound portions of  $^{18}\text{FMB}$  were present in the radioligand solution, and the free radioligand concentration as such entered into the saturation binding analysis.

A further problem arises from the lack of concurrent morphologic imaging and the consequent impossibility of exactly determining the stereotactic coordinates of the PET slices on which the striatal ROIs were delineated. As a consequence, PET and autoradiography evaluation may not have corresponded as to the anteroposterior sectional plane. Because there are regional differences in the distribution of binding sites (18), this lack of correspondence may explain the difference between receptor densities obtained with the 2 methods. Moreover, phantom studies previously performed with our small-animal tomograph (2) have shown that in a target with a diameter of 2.5 mm (i.e., in the range of the striatal diameters on the coronal slices used for ROI definition), radioactivity was underestimated by approximately 60% on account of the partial-volume effect. On the basis of these measurements, striatal radioactivity concentrations were corrected. The used correction factor, however, was the same for all experiments and not exactly determined for the actual striatal diameter on the slice selected for ROI definition. If the striatal diameter had fallen below 2.5 mm, the used correction factor would have led to an underestimation of radioactivity concentration, compared with the concentration determined by autoradiography. This may have been the case, since slices were selected not only with respect to the localization of the striatal activity maxima but also with the intent to minimize spillover from the adjacent retroorbital tissue. As a consequence, ROIs were placed within the intermediate-to-caudal portion of the striatum.

In the present study,  $K_d$  values agreed whereas  $B_{\max}$  values merely lay in the same order of magnitude. Placement of ROIs necessarily influences  $B_{\max}$ , whereas  $K_d$  remains the same for all receptors of the same subtype irrespective of the striatal portion selected for ROI definition. In contrast, inaccurate determinations of the free radioligand concentrations influence both  $B_{\max}$  and  $K_d$ . Because  $K_d$  values agreed in our experiments, we may conclude that incongruent ROI placement exerted the more prominent effect on our assessment of receptor kinetics.

Our approach is novel in that it allows the performance of in vivo saturation binding studies in analogy to in vitro experiments. Receptor kinetics may be assessed in the living animal instead of using cryosections or membrane homogenates as mere models of cerebral tissue and receptor surface. Because the present validation study showed good agreement between in vivo and in vitro results, it will be possible to reduce the numbers of animal used in future investigations. Because the PET methodology allows repeated investigations of the same animal, various radioligand concentrations can be tested in a single rat, provided that the measurements lie a sufficient time apart. Otherwise, data acquisition might be compromised by residual  $^{18}\text{FMB}$  or tracer metabolites originating from precedent measurements. In contrast, in our autoradiographic study, 4–6 animals were sacrificed per data point to handle the problem of interindividual variance. Thus, in vivo saturation binding

analysis not only has the benefit of minimizing this problem by reducing the number of experimental rats per molar concentration but also takes into account the German Law on the Protection of Animals.

## CONCLUSION

The  $K_d$  values of receptor binding data obtained with PET and with storage phosphor autoradiography agreed well and corresponded to inhibition constants obtained with homogenized rat striata in previous studies.  $B_{max}$  values lay within the same order of magnitude. Moreover, the results of in vitro saturation binding analysis agreed irrespective of whether the nonspecific binding had been estimated from cortical radioactivity concentrations, as was done in the evaluation of in vivo data, or from joint incubation with the radioligand and a highly selective competitor. As a consequence,  $K_d$  and  $B_{max}$  may be determined with PET in analogy to the evaluation of in vitro binding data with nonlinear or linear regression analysis of free-versus-bound ligand concentrations. This permits the in vivo characterization of novel receptor radioligands under physiologic conditions with PET devices suitable for the investigation of small laboratory animals.

## ACKNOWLEDGMENTS

This work was supported by a grant from the Forschungskommission of the Faculty of Medicine, Heinrich-Heine-Universität, Düsseldorf, Germany. The authors acknowledge Markus Cremer, Heinz Mühlensiepen, and Sabine Wilms from the Institut für Medizin, as well as Dr. Simone Weber from the Zentrallabor für Elektronik (Forschungszentrum Jülich GmbH), for their contributions to the experiments.

## REFERENCES

1. Weber S, Terstege A, Herzog H, et al. The design of an animal PET: flexible geometry for achieving optimal spatial resolution or high sensitivity. *IEEE Trans Med Imaging*. 1997;16:684–698.
2. Nikolaus S, Larisch R, Beu M, Vosberg H, Müller-Gärtner HW. Imaging of striatal dopamine  $D_2$  receptors with a PET system for small laboratory animals in comparison with storage phosphor autoradiography: a validation study with [ $^{18}F$ ](3-N-methyl)benperidol. *J Nucl Med*. 2001;42:1691–1696.
3. Hume SP, Myers R, Bloomfield PM, et al. Quantitation of carbon-11-labeled raclopride in rat striatum using positron emission tomography. *Synapse*. 1992;12:47–54.
4. Hume SP, Opacka-Juffry, Myers R. Effect of L-dopa and 6-hydroxydopamine

lesioning on [ $^{11}C$ ]raclopride binding in rat striatum, quantified using PET. *Synapse*. 1995;21:45–53.

5. Tsukada H, Kreuter J, Maggos CE, et al. Effects of binge cocaine administration on dopamine  $D_1$  and  $D_2$  receptors in the rat brain: an in vivo study using positron emission tomography. *J Neurosci*. 1996;16:7670–7677.
6. Unterwald EM, Tsukada H, Kakiuchi T, Kosugi T, Nishiyama S, Kreek MJ. Use of positron emission tomography to measure the effect of nalmefene on  $D_1$  and  $D_2$  dopamine receptors in rat brain. *Brain Res*. 1997;775:183–188.
7. Ishiwata K, Hayakawa N, Ogi N, et al. Comparison of three PET dopamine  $D_2$ -like receptor ligands, [ $^{11}C$ ]raclopride, [ $^{11}C$ ]nemonapride and [ $^{11}C$ ]N-methylspiperone, in rats. *Ann Nucl Med*. 1999;13:161–167.
8. Suzuki M, Hatano K, Sakiyama Y, Kawasumi Y, Kato T, Ito K. Age-related changes of dopamine  $D_1$ -like and  $D_2$ -like receptor binding in the F344/N rat striatum revealed by positron emission tomography and in vitro receptor autoradiography. *Synapse*. 2001;41:285–293.
9. Umegaki H, Ishiwata K, Ogawa O, et al. In vivo assessment of adenoviral vector-mediated gene expression of dopamine  $D_2$  receptors in the rat striatum by positron emission tomography. *Synapse*. 2002;43:195–200.
10. Moerlein SM, Banks WR, Parkinson D. Production of fluorine-18 labeled (3-N-methyl)benperidol for PET investigation of cerebral receptor binding. *Appl Radiat Isot*. 1992;43:913–917.
11. Hamacher K, Hamkens W. Remote controlled one-step production of  $^{18}F$  labeled butyrophenone neuroleptics exemplified by the synthesis of n. a. c. [ $^{18}F$ ]N-methylspiperone. *Appl Radiat Isot*. 1995;46:911–916.
12. Moerlein SM, Perlmutter JS, Welch MJ. Specific, reversible binding of [ $^{18}F$ ]benperidol to baboon  $D_2$  receptors: PET evaluation of an improved  $^{18}F$ -labeled ligand. *Nucl Med Biol*. 1995;22:809–815.
13. Digenis GA, Vincent SH, Kook CS, Reiman RE, Russ GA, Tilbury RS. Tissue distribution studies of [ $^{18}F$ ]haloperidol, [ $^{18}F$ ]- $\beta$ -[4-fluorobenzoyl]propionic acid, and [ $^{82}Br$ ]bromperidol by external scintigraphy. *J Pharm Sci*. 1981;70:985–989.
14. Paxinos G, Watson C. *The Rat Brain in Stereotaxic Coordinates*. Sydney, Australia: Academic Press; 1986:19–28.
15. Ito H, Hietala J, Blomqvist G, Halldin C, Farde L. Comparison of the transient equilibrium and continuous infusion method for quantitative PET analysis of [ $^{11}C$ ]raclopride binding. *J Cereb Blood Flow Metab*. 1998;18:941–950.
16. Beu M, Nikolaus S, Larisch R, Weber S, Vosberg H, Müller-Gärtner HW. An algorithm to quantify the influence of Harder's glands on striatal radioactivity in PET measurements of rats [abstract, in German]. *Nuklearmedizin*. 2000;39:162.
17. Kessler RM, Ansari MS, Schmidt DE, et al. High affinity dopamine  $D_2$  receptor radioligands. 2. [ $^{125}I$ ]Epididone, a potent and specific radioligand for the characterization of striatal and extrastriatal dopamine  $D_2$  receptors. *Life Sci*. 1991;49:617–628.
18. Lidow MS, Goldman-Rakic PS, Rakic P, Innis RB. Dopamine  $D_2$  receptors in the cerebral cortex: distribution and pharmacological characterization with [ $^3H$ ]raclopride. *Proc Natl Acad Sci USA*. 1989;86:6412–6416.
19. Ito T, Suzuki T, Lim DK, Wellman SE, Ho IK. A novel quantitative receptor autoradiography and in situ hybridization histochemistry technique using storage phosphor screen imaging. *J Neurosci Meth*. 1995;59:265–271.
20. Suehiro M, Dannals RF, Scheffel U, et al. In vivo labeling of the dopamine  $D_2$  receptor with N- $^{11}C$ -methyl-benperidol. *J Nucl Med*. 1990;31:2015–2021.
21. Moerlein SM, Perlmutter JS. Specific binding of 3N-(2[ $^{18}F$ ]fluoroethyl)benperidol to primate cerebral dopaminergic  $D_2$  receptors demonstrated in vivo by PET. *Neurosci Lett*. 1992;148:97–100.
22. Moerlein SM, Perlmutter JS, Markham J, Welch MJ. In vivo kinetics of [ $^{18}F$ ](N-methyl)benperidol: a novel PET tracer for assessment of dopaminergic  $D_2$ -like receptor binding. *J Cereb Blood Flow Metab*. 1997;17:833–845.
23. Hume SP, Lammertsma AA, Myers R, et al. The potential of high-resolution positron emission tomography to monitor striatal dopaminergic function in rat models of disease. *J Neurosci Meth*. 1996;67:103–112.



SOCIETY OF  
NUCLEAR  
MEDICINE